Effect of aperture field distribution on the maximum radiated power at atmospheric pressure*

Pengcheng Zhao(赵朋程)† and Lixin Guo(郭立新)

School of Physics and Optoelectronic Engineering, Xidian University, Xi'an 710071, *China*

(Received 23 June 2017; revised manuscript received 19 July 2017; published online 30 September 2017)

The air breakdown in the high-power antenna near-field region limits the enhancement of the radiated power. A model coupling the field equivalent principle and the electron number density equation is presented to study the breakdown process in the near-field region of the circular aperture antenna at atmospheric pressure. Simulation results show that, although the electric field in the near-field region is nonuniform, the electron diffusion has small influence on the breakdown process when the initial electron number density is uniform in space. The field magnitude distribution on the aperture plays an important role in the maximum radiated power above which the air breakdown occurs. The maximum radiated power also depends on the phase difference of the fields at the center and edge of the aperture, especially for the uniform field magnitude distribution.

Keywords: field equivalent principle, aperture antenna, air breakdown, maximum radiated power

PACS: 51.50.+v, 92.60.Ta **DOI:** 10.1088/1674-1056/26/11/115101

1. Introduction

The high-power microwave has important applications in many fields, such as the long-distance wireless energy transport, creation of ionospheric and atmospheric ducts for long-range communications, high-power radar systems, and plasma chemistry.[1] In recent years, the electric field radiated from the aperture antenna reaches several MV/m that can exceed the breakdown electric field at atmospheric pressure.[2,3] Once the air breakdown occurs, the attendant plasma strongly hinders the microwave radiation. This suggests that the radiated power reaches the maximum (or critical) value when the maximum electric field in the near-field region is equal to the breakdown electric field. Therefore, it is very important to study and understand the maximum radiated power limited by the air breakdown.

The air breakdown caused by the high-power microwave has been investigated by many scholars in recent years.[4–9] Hidaka *et al.* observed the variation of the plasma pattern produced in the air breakdown with the pressure, which was well reproduced and explained by the theory model of Boeuf *et al.*[4,5] Experiments of Yang *et al.* showed that the breakdown threshold of the short-pulse microwave depends strongly on the gas pressure and species.[6] The electron fluid model with the accurate rate coefficients was employed by Zhao *et al.* to simulate and reveal the air breakdown caused by the high-power microwave.[7,8] In general, we do not desire the air breakdown to occur, and therefore determining the maximum radiated power above which the air breakdown occurs is important to avoid the breakdown. The field equivalent principle and the empirical formula of the ionization rate were employed by Zhang *et al.* to study the maximum radiated power of the aperture antenna, where the field phase on the aperture was assumed to be uniform.[9] However, the field phase on the aperture can be nonuniform, which has an important impact on the pattern of the radiated field. It can also be expected that the maximum radiated power changes with the field phase distribution.

In this paper, we study the air breakdown process in the near-field region of the circular aperture antenna at atmospheric pressure using a model coupling the field equivalent principle with the electron number density equation. The electron diffusion that may have an influence on the breakdown process in the nonuniform field is included in the electron number density equation. We first simulate the evolution of the electron number density in the breakdown process, and show how the electron ionization, attachment, and diffusion affect the evolution. Then we focus on the dependence of the maximum radiated power on the field phase and magnitude distribution on the aperture.

2. Model

The plasma produced in the air breakdown process has little influence on the incident microwave until its number density reaches the critical value $n_c \approx (\varepsilon_0 m_e/q_e^2)\omega^2$, where ε_0 is the permittivity of free space, ω is the angular frequency of the microwave, and m_e and q_e denote the charge and mass of

*Project supported by the National Natural Science Foundation of China (Grant Nos. 61501358, 11622542, 61431010, and 61627901) and the Fundamental Research Funds for the Central Universities, China.

†Corresponding author. E-mail: pczhao@xidian.edu.cn

© 2017 Chinese Physical Society and IOP Publishing Ltd

electron, respectively.[10] In this paper, we focus only on the process before air breakdown and predict the maximum power radiated from the circular aperture antenna above which the air breakdown occurs. We first adopt the field equivalent principle to solve the radiated electric field in the near-field region, which can be approximated as a free space. Then we use the electron number density equation to describe the evolution of the electron number density in the breakdown process. Finally, the definition of the maximum radiated power is presented.

2.1. Field equivalence principle

The equivalent electric current on the aperture alone can be written as[11]

$$\boldsymbol{J}_{\mathrm{e}} = -2\boldsymbol{E}_{\mathrm{a}}/\eta_0, \tag{1}$$

where $\boldsymbol{E}_{\mathrm{a}}$ is the electric field on the aperture and η_0 is the wave impedance of the free space. The vector potential corresponding to the electric current is given by

$$\begin{aligned}\boldsymbol{A}(\boldsymbol{r},\omega) &= -\frac{\mu_0}{2\pi\eta_0}\int_{s'}\left[\boldsymbol{e}_x E_{x\mathrm{a}}(\boldsymbol{r}',\omega)+\boldsymbol{e}_y E_{y\mathrm{a}}(\boldsymbol{r}',\omega)\right]\\ &\quad\times\frac{\mathrm{e}^{-\mathrm{j}kR}}{R}\,\mathrm{d}S',\end{aligned} \tag{2}$$

where $k=\omega\sqrt{\varepsilon_0\mu_0}$ is the wave number, μ_0 is the permeability of the free space, and R is the distance between the field point $\boldsymbol{r}$ and the source point $\boldsymbol{r}'$. By using Eq. (2), the radiated fields can be obtained as follows:

$$\begin{aligned}\boldsymbol{H}(\boldsymbol{r}) &= \frac{1}{\mu_0}\nabla\times\boldsymbol{A}(\boldsymbol{r},\omega)\\ &= \frac{1}{2\pi\eta_0}\int_{s'}\mathrm{e}^{-\mathrm{j}kR}\left(\frac{\mathrm{j}k}{R^2}+\frac{1}{R^3}\right)\\ &\quad\times\left\{-\boldsymbol{e}_x z E_{y\mathrm{a}}+\boldsymbol{e}_y z E_{x\mathrm{a}}\right.\\ &\quad\left.+\boldsymbol{e}_z\left[(x-x')E_{y\mathrm{a}}-(y-y')E_{x\mathrm{a}}\right]\right\}\mathrm{d}S',\end{aligned} \tag{3}$$

$$\begin{aligned}\boldsymbol{E}(\boldsymbol{r}) &= \frac{1}{\mathrm{j}\omega\varepsilon_0}\nabla\times\boldsymbol{H}(\boldsymbol{r},\omega)\\ &= \frac{1}{\mathrm{j}2\pi\omega\varepsilon_0\eta_0}\int_{s'}\left\{2\left(\frac{-\mathrm{j}k}{R^2}-\frac{1}{R^3}\right)(\boldsymbol{e}_x E_{x\mathrm{a}}+\boldsymbol{e}_y E_{y\mathrm{a}})\right.\\ &\quad+\left(\frac{-k^2}{R^3}+\frac{\mathrm{j}3k}{R^4}+\frac{3}{R^5}\right)\\ &\quad\times\left\{\boldsymbol{e}_x\left\{E_{x\mathrm{a}}\left[(y-y')^2+z^2\right]-E_{y\mathrm{a}}(x-x')(y-y')\right\}\right.\\ &\quad+\boldsymbol{e}_y\left\{E_{y\mathrm{a}}\left[(x-x')^2+z^2\right]-E_{x\mathrm{a}}(x-x')(y-y')\right\}\\ &\quad\left.\left.-\boldsymbol{e}_z\left[E_{x\mathrm{a}}(x-x')z+E_{y\mathrm{a}}(y-y')z\right]\right\}\right\}\mathrm{e}^{-\mathrm{j}kR}\mathrm{d}S'.\end{aligned} \tag{4}$$

2.2. Electron number density equation

Considering the fact that the radiated electric field in the near-region is nonuniform, the electron diffusion term is included in the electron number density equation. Since we focus on the process in which the electron number density grows from the initial level to the critical value above which the incident wave is disturbed, the electron number density is low and then the electron–ion recombination can be ignored. Therefore, the electron number density can be expressed as[12]

$$\frac{\partial n_{\mathrm{e}}}{\partial t} = (\nu_{\mathrm{i}}-\nu_{\mathrm{a}})n_{\mathrm{e}}+D_{\mathrm{eff}}\nabla^2 n_{\mathrm{e}}, \tag{5}$$

where n_{e} denotes the electron number density, ν_{i} and ν_{a} are the ionization rate and attachment rate, respectively, and D_{eff} is the effective electron diffusion coefficient.

The ν_{i} and ν_{a} are obtained from the following empirical scaling laws:[12]

$$\frac{\nu_{\mathrm{i}}}{p} = 5\times10^4\left(\frac{E_{\mathrm{eff}}}{E_{\mathrm{c}}}\right)^{5.33}, \tag{6}$$

$$\frac{\nu_{\mathrm{a}}}{p} = 5\times10^4, \tag{7}$$

where p is the air pressure, $E_{\mathrm{c}}\approx 3200p$ is the critical field at which the ionization balances the attachment, and E_{eff} is the effective electric field. Note that equation (6) holds only when $E_{\mathrm{eff}}/E_{\mathrm{c}}$ lies between 1 and 3. E_{eff} can be written as

$$E_{\mathrm{eff}} = E_{\mathrm{rms}}\left(1+\omega^2/\nu_{\mathrm{m}}^2\right)^{1/2}, \tag{8}$$

where the collision frequency ν_{m} is approximated as

$$\frac{\nu_{\mathrm{m}}}{p} = 5.3\times10^9. \tag{9}$$

D_{eff} is expressed as[5]

$$D_{\mathrm{eff}} = \frac{\alpha D_{\mathrm{e}}+D_{\mathrm{a}}}{\alpha+1}, \tag{10}$$

$$\alpha = \frac{\nu_{\mathrm{i}}\varepsilon_0}{q_{\mathrm{e}}N_{\mathrm{e}}\left(\mu_{\mathrm{e}}+\mu_{\mathrm{i}}\right)}, \tag{11}$$

where α is the local Maxwell relaxation time, $\mu_{\mathrm{e}}=q_{\mathrm{e}}/m_{\mathrm{e}}\nu_{\mathrm{m}}$ and $\mu_{\mathrm{i}}=\mu_{\mathrm{e}}/200$ are the electron mobility and ion mobility, respectively, $D_{\mathrm{a}}=(\mu_{\mathrm{i}}/\mu_{\mathrm{e}})D_{\mathrm{e}}$ is the ambipolar diffusion coefficient, $D_{\mathrm{e}}=\mu_{\mathrm{e}}T_{\mathrm{e}}/e$ is the free diffusion coefficient, and the electron temperature T_{e} is approximated as[12]

$$T_{\mathrm{e}} = \left[2.1\times10^{-3}\frac{E_{\mathrm{eff}}}{p}\left(91+\frac{E_{\mathrm{eff}}}{p}\right)\right]^{1/3}. \tag{12}$$

Note that equation (12) is valid only when $E_{\mathrm{eff}}/p \le 100\ \mathrm{V\cdot cm^{-1}\cdot Torr^{-1}}$.

2.3. Maximum radiated power

When the electron diffusion term can be ignored, integration of Eq. (5) yields

$$n_{\mathrm{e}}(t) = n_{\mathrm{e}0}\exp\left[\left(\nu_{\mathrm{i}}-\nu_{\mathrm{a}}\right)t\right], \tag{13}$$

where $n_{\mathrm{e}0}$ is the initial electron number density. The electron number density grows exponentially and the breakdown is defined to occur when the density has increased to the critical level above which the microwave is disturbed obviously by

the breakdown plasma.[5] Under the breakdown electric field, equation (13) can be rewritten as

$$n_{\mathrm{e}}(t_{\mathrm{p}}) = n_{\mathrm{e}0}\exp\left[\left(\nu_{\mathrm{i}}-\nu_{\mathrm{a}}\right)t_{\mathrm{p}}\right] = n_{\mathrm{c}}, \tag{14}$$

where t_{p} is the microwave pulse width. By introducing Eqs. (6)–(8) into Eq. (14), the rms breakdown electric field is obtained as follows:

$$E_{\mathrm{b}} = \left[\frac{\ln\left(n_{\mathrm{c}}/n_{\mathrm{e}0}\right)}{5\times10^4 p t_{\mathrm{p}}}+1\right]^{\frac{1}{5.33}}\left(\frac{\nu_{\mathrm{m}}^2}{\nu_{\mathrm{m}}^2+\omega^2}\right)^{-1/2}E_{\mathrm{c}}. \tag{15}$$

Let $t_{\mathrm{p}}\to\infty$ in Eq. (15), the rms breakdown electric field for the continuous microwave can expressed as

$$E_{\mathrm{b}} = \left(\frac{\nu_{\mathrm{m}}^2}{\nu_{\mathrm{m}}^2+\omega^2}\right)^{-1/2}E_{\mathrm{c}}. \tag{16}$$

When the effect of the electron diffusion on the breakdown process is obvious, we must adopt Eq. (5) to determine E_{b}.

The power density corresponding to the breakdown electric field is

$$P_{\mathrm{b}} = \mathrm{Re}(\boldsymbol{E}\times\boldsymbol{H}^*)/2, \tag{17}$$

where '*' represent the conjugate operation, and $|\boldsymbol{E}| = E_{\mathrm{b}}$. When the maximum radiated power density reaches P_{b}, the antenna radiated power approaches the upper limit

$$P_{\max} = \frac{P_{\mathrm{b}}}{\gamma_{\max}^2}\int_{S'}|\overline{E}_{\mathrm{a}}(r')|^2\,\mathrm{d}S', \tag{18}$$

where $\gamma_{\max}$ is the ratio of the maximum radiated electric field to the maximum aperture electric field, $\overline{E}_{\mathrm{a}}(r')$ is the normalized electric field on the aperture, and S' is the aperture. It is clear that $\gamma_{\max}\geq 1$.

3. Results and discussion

The air pressure is taken as 760 Torr that corresponds to one atmospheric pressure. At the initial time, the electron number density $n_{\mathrm{e}0} = 1\times10^6\ \mathrm{m}^{-3}$ is uniform in the near-field region. The circular aperture with the radius of 0.2 m is placed on the x–y plane, whose center is located at the origin of the coordinate system. It is assumed that the microwave electric field on the aperture has one component, i.e., $\boldsymbol{E}_{\mathrm{a}} = \boldsymbol{e}_x E_{x\mathrm{a}}$. When the field distribution on the aperture is taken to be cylindrical symmetric, the field radiated from the aperture is also cylindrical symmetric. Therefore, the three-dimensional problem can be reduced into a two-dimensional one and we can consider only the electric field and the electron number density on the yoz plane. We focus on the breakdown prediction of the continuous microwave with a frequency of 2.85 GHz. The microwave is a monochromatic wave, whose magnetic and electric field can be directly solved by Eqs. (3) and (4).

Figure 1 shows the electric field radiated from the aperture on which the phase and magnitude of the field are uniform. It is obvious that the radiated field is nonuniform. When the maximum radiated field is taken to be slightly higher than the critical field E_{c}, for example, $1.1E_{\mathrm{c}}$, the evolution of the electron number density is simulated, as shown in Figs. 2 and 3. In the high field region, the ionization rate is larger than the rate of electron loss due to the attachment and diffusion, so the electron number density at 50 ns in Fig. 2(a) shows an obvious increase compared with the initial one. We also find that, with further increase in time, the electron number density in the high field region becomes higher, while its profile is similar to the one at $t = 50$ ns, as shown in Fig. 2(b). This is because the electron diffusion is much less than the electron ionization and attachment, as shown in Fig. 3. The phenomenon is also observed at other aperture field distributions. The secondary electron emission is not considered. This is because at a high pressure the mean secondary emission yield is much lower than unity, and the ionization becomes the dominant mechanism to generate electrons.[13]

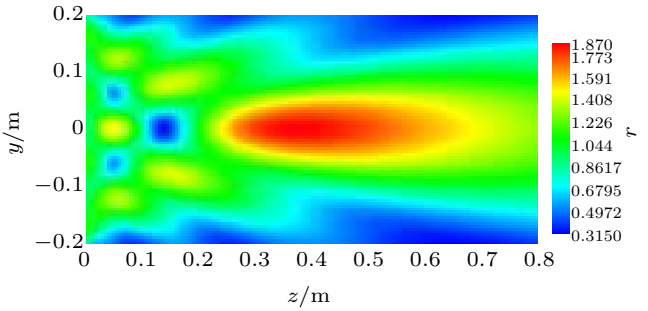


Fig. 1. (color online) The ratio of radiated electric field to maximum aperture electric field. The phase and magnitude of the field on the aperture are uniform.

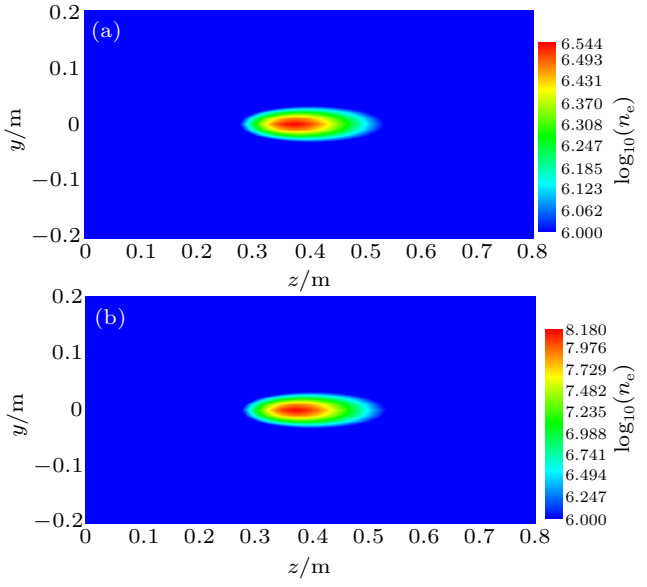


Fig. 2. (color online) The spatial distribution of the electron number density at $t = 50$ ns (a) and 200 ns (b) under the radiated field corresponding to Fig. 1. The maximum radiated electric field is equal to $1.1E_{\mathrm{c}}$.

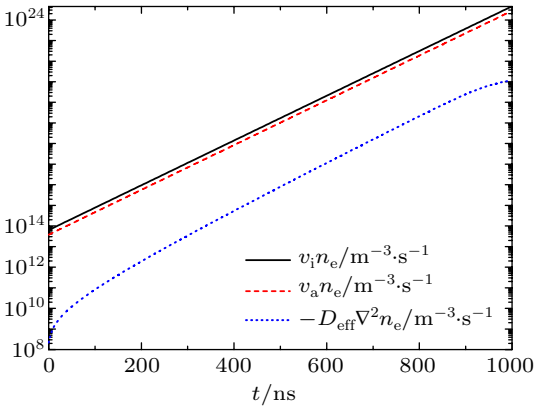


Fig. 3. (color online) Comparison among electron ionization, attachment, and diffusion at the point where the radiated field is maximum. The radiated field profile corresponds to Fig. 1 and its maximum value is equal to $1.1E_c$.

We consider three different distributions of the aperture field magnitude, which are the uniform, parabolic taper with pedestal, and parabolic taper distributions, respectively.[11] The distributions of parabolic taper with pedestal and parabolic taper can be written as follows:

$$|\overline{E}_a(r')| \propto 0.3+0.7\left[1-\left(r'/a\right)^2\right], \tag{19}$$

$$|\overline{E}_a(r')| \propto 1-\left(r'/a\right)^2. \tag{20}$$

The field phase on the aperture is assumed as

$$\phi(r') = -\left(r'/a\right)^2 \phi_{max}, \tag{21}$$

where ϕ_{max} is the phase difference of the fields at the center and edge of the aperture. Figure 4 shows the ratio γ_{max} of the maximum radiated electric field to the maximum aperture electric field for the three different aperture field distributions. It can be seen from this figure that the field magnitude distribution plays an important role on γ_{max}. Of the three field magnitude distributions, γ_{max} corresponding to the uniform field magnitude distribution is highest. γ_{max} for the uniform field magnitude distribution depends obviously on the phase difference ϕ_{max}, while for the other two field magnitude distributions, the dependence appears only at $\phi_{max} < \pi$.

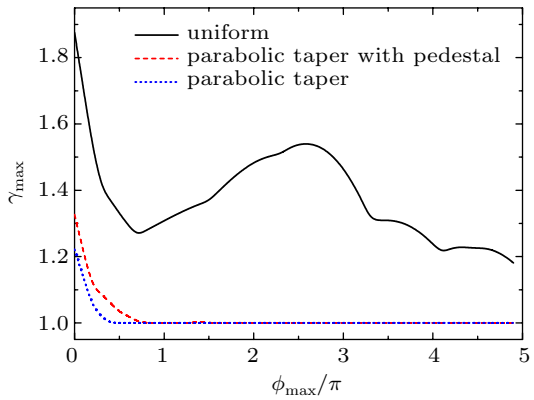


Fig. 4. (color online) The ratio of maximum radiated electric field to maximum aperture electric field for three different aperture field distributions.

Figure 5 shows the maximum radiated power above which the air breakdown occurs. The aperture field distributions can refer to Eqs. (19)–(21). Since the electron diffusion has small influence on the breakdown process (see Fig. 3), equation (16) can be adopted to predict the breakdown electric field E_b. Under the fixed air pressure and field magnitude distribution, E_b remains unchanged, and $P_{max} \propto 1/\gamma_{max}^2$ (see Eq. (18)). Therefore, the variation of P_{max} with ϕ_{max} has a contrary trend with that of γ_{max}, as shown in Figs. 4 and 5. Of the three different field magnitude distributions, both γ_{max} and $\int_{S'} |\overline{E}_a(r')|^2 \mathrm{d}S'$ corresponding to the uniform field magnitude distribution are highest. As a result, the corresponding P_{max} is highest around $\phi_{max} = 2.5\pi$.

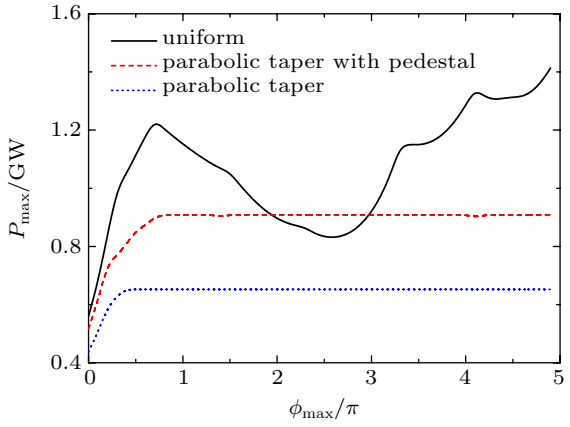


Fig. 5. (color online) The maximum radiated powers for three different aperture field distributions.

To validate the breakdown prediction, the breakdown thresholds obtained from Eq. (15) are compared with the experiment results of Cook *et al.* (see Ref. [14]) under $f = 110$ GHz and $t_p = 2500$ ns, as shown in Fig. 6. It can be seen from this figure that the breakdown prediction agrees very well the experimental data. The fluctuation in the experimental data is caused by the seed electrons.[2]

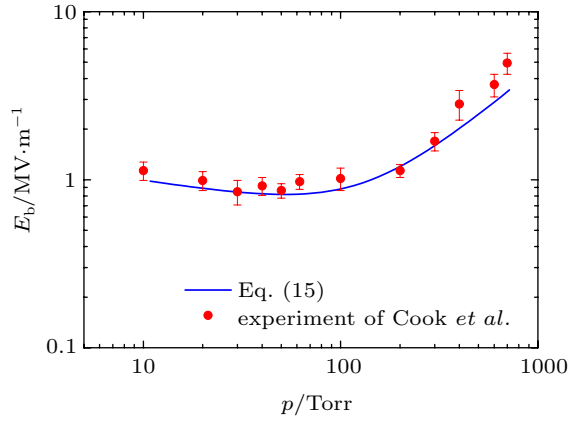


Fig. 6. (color online) Breakdown thresholds obtained from Eq. (15) and experiments of Cook *et al.* under $f = 110$ GHz and $t_p = 2500$ ns.

4. Conclusion

The model coupling the field equivalent principle and the electron number density equation is presented to study the air breakdown process in the near-field region of the circular aperture antenna, and to predict the maximum radiated power above which the air breakdown occurs. The terms of the electron ionization, attachment, and diffusion are included in the electron number density equation. The magnitude of the aperture field is assumed to have the uniform, parabolic taper with pedestal, and parabolic taper field distributions, respectively, and its phase is nonuniform. The results show that, although the electric field in the near-field region is nonuniform, the electron diffusion has small influence on the breakdown process when the initial electron number density is uniform in space. The distribution of the aperture field magnitude plays an important role in the maximum radiated power. The maximum radiated power for the uniform field magnitude distribution depends on the phase difference of the fields at the center and edge of the aperture, while for the other two field magnitude distributions, the dependence appears only at small phase differences.

References

[1] Golubev A I, Sysoeva T G, Terekhin V A, Tikhonchuk V T and Altgilbers L L 2000 *IEEE Trans. Plasma Sci.* **28** 303

[2] Ford P J, Beeson S R, Krompholz H G and Neuber A A 2012 *Phys. Plasmas* **19** 073503

[3] Chang C, Verboncoeur J, Wei F L, Xie J L, Sun J, Liu Y S, Liu C L and Wu C 2017 *IEEE Trans. Dielectr. Electr. Insul.* **24** 375

[4] Hidaka Y, Choi E M, Mastovsky I, Shapiro M A, Sirigiri J R and Temkin R J 2008 *Phys. Rev. Lett.* **100** 035003

[5] Boeuf J P, Chaudhury B and Zhu G Q 2010 *Phys. Rev. Lett.* **104** 015002

[6] Yang Y, Yuan C and Qian B 2012 *Phys. Plasmas* **19** 122101

[7] Zhao P, Guo L and Li H 2015 *Chin. Phys. B* **24** 105102

[8] Zhao P, Guo L and Shu P 2017 *Chin. Phys. B* **26** 029201

[9] Zhang J and Wang J 2011 *IEEE Electromagn. Compat.* **53** 540

[10] Zhao P, Liao C and Feng J 2015 *Chin. Phys. B* **24** 025101

[11] Stutzman W L and Thiele G A 1998 *Antenna Theory and Design* (2nd Edn.) (New York: Wiley) pp. 275–283

[12] Zhu G Q, Boeuf J P and Chaudhury B 2011 *Plasma Sources Sci. Technol.* **20** 035007

[13] Kim H C and Verboncoeur J P 2006 *Phys. Plasmas* **13** 123506

[14] Cook A, Shapiro M and Temkin R 2010 *Appl. Phys. Lett.* **97** 011504